Research Square

Preprints are preliminary reports that have not undergone peer review.
They should not be considered conclusive, used to inform clinical practice,
or referenced by the media as validated information.

# Stochastic and deterministic evolutionary processes in microecosystem of dye-degrading functional microbiomes

**XIN Liu**
Donghua University
**Yiting Qin**
Donghua University
**Jiajie Liu**
Donghua University
**Wanting Li**
Donghua University
**Xinyi Guo**
Donghua University
**Na Liu**
Suzhou University
**Qingyun Zhang**
Anhui Polytechnic University
**Xuehui Xie**
xiexuehui@dhu.edu.cn
Donghua University
**Ye Chen**
Donghua University

**Article**

**Keywords:** Functional microbiome, Microbiome evolution, Activator, Electron donor, Degradation decolorization

**Posted Date:** May 12th, 2026

**DOI:** https://doi.org/10.21203/rs.3.rs-9048998/v1

**License:** This work is licensed under a Creative Commons Attribution 4.0 International License.
Read Full License

**Additional Declarations:** No competing interests reported.

# Abstract

Dye wastewater seriously damages the water ecosystem and threatens human health. Functional microbiome showed significant advantages in dye wastewater treatment with their excellent degradation ability. The evolution of the microbiome has important implications for its functionality. The study provided insights into the evolutionary mechanisms of functional microbiome in dye wastewater treatment, based on research data spanning from 2015 to 2024. It was found that the changes of environmental factors had a great influence on the structure of microbiome, which was dominated by stochastic evolution in the short term. However, long-term follow-up monitoring showed that the functional microbiome was dominated by deterministic evolution, displaying good stability and adaptability. In addition, it was worth noting that interannual evolution of the microbiome was mainly influenced by biological interactions, whereas the intra-annual evolutionary process was mainly dominated by environmental selection. These results provide more efficient, stable and reliable biological solutions to environmental problems such as wastewater treatment.


# Introduction

Globally, the printing and dyeing industry has consistently been an important manufacturing sector. Dye wastewater therefrom has a high chroma and contains a considerable amount of organic pollutants, which not only significantly affects the appearance of the receiving water body but also undermines the aquatic ecological environment[1, 2]. The demand of people for a beautiful ecological environment urges the effective treatment of dye wastewater to be more urgent[3]. Biological methods are often used in the treatment of dye wastewater because of their low consumption, environmental protection and high efficiency[4]. The functional microbiome, with its exceptional biodegradability and environmental adaptability, demonstrates considerable advantages in the biological treatment of dye wastewater[5, 6]. Functional microbiome is a complex microecosystem containing several different communities that work together to fulfil specific functions. Therefore, an in-depth understanding of microbiology in process of dye decolorization is crucial.

Artificially domesticated functional microbiome usually undergoes some degree of selection and guidance, and is therefore characterised by a degree of deterministic evolution[7]. In adapting to a particular environment or fulfilling a particular function, functional microbiome may undergo a series of deterministic evolutionary processes to adapt to the ecological niche in which they are found and to fulfil a particular function[8]Human intervention can be used to induce certain microbiome to gain an advantage and multiply in response to human intervention by selecting specific microorganisms, providing specific growth conditions, and so on, in order to fulfil specific functions[9]. The process of such interventions is usually purposeful and planned, and therefore to some extent deterministic. However, there can also be a degree of randomness in the process of human intervention[7]. For example, environmental factors, competitive pressures, mutations and other factors may affect the process of evolution and development of the microbiome, leading to some stochastic changes[10]. Thus,

although artificially domesticated functional microbiome is characterised by deterministic evolution, a degree of stochasticity may still be present in the evolutionary process. Determinism and stochasticity are intertwined in the evolution of functional microbiome. Together, they shape the microbiome's diversity and adaptability, ultimately influencing its functionality.

Currently, there is a lack of studies on deterministic as well as stochastic evolution of functional microbiome. Functional microbiome had shown great potential in treating environmental problems such as dye wastewater. However, to make full use of these microbiome, an in-depth understanding of their evolutionary mechanisms and modes of regulation is required. In terms of deterministic evolution, a large number of studies have clarified the optimal growth environments for many functional microbiome, as well as their reproductive metabolic processes[11, 12]However, the multiple dimensions of the regulatory network within the microbiome and the interactions between the colonies require more research to reveal the underlying mechanisms. At the same time, there is insufficient understanding of how these factors affect the evolution of functional microbiome and how they can be controlled and utilised[13, 14].

In order to better understand the microbial interactions of functional communities during dye wastewater treatment and to reveal the mechanism of natural microbiome construction, this study collected a large amount of functional microbiome data during a total of ten years of research experiments from 2015 to 2024. The effects of anthropogenic disturbances such as stress domestication, addition of exotic substances, etc. were assessed on the properties of functional microbial interactions networks associated with the degradation of dye wastewater. The study is based on zero modelling with phylogenetic data to access community structure assembly processes and uses an analytical framework to quantify the relative roles of deterministic and stochastic processes. Based on Spearman's correlation coefficient, a correlation network was constructed to explore the co-existing relationships among microorganisms. Two important node characteristics, intra-module connectivity and inter-module connectivity, are derived on the basis of network modules, and node attributes can be classified into four types based on the topological characteristics of the nodes to find key species in the microbial association network. These results help to understand how complex functional microbiome respond to and recover from long-term anthropogenic disturbances, assess their relationship with dye wastewater treatment, and further reveal the mechanisms of evolutionary succession of microbiome during dye wastewater treatment. Through more in-depth research, we are expected to better understand the evolutionary laws of functional bacterial microbiome and provide more efficient, stable and reliable biological solutions to environmental problems such as wastewater treatment.

# 1. Materials and methods

## 1.1. Chemicals, culture media and microbiome

Remazol Brilliant Blue R (RBBR/RB19, CAS No.2580-78-1, MW 626.54), Reactive black 5 (RB5, CAS No. 17095-24-8, MW 991.82), Acid Orange 7 (AO7, CAS No.633-96-5, MW 350.32), Chorazol Black E (CBE,

CAS No.1937-37-7, MW 781.73) and Malachite Green (MG CAS No.2437-29-8, MW 463.5) were purchased from Sigma-Aldrich (USA). All inorganic salts were purchased from Sinopharm Chemical Reagent (Shanghai) Co., Ltd. Yeast extract was purchased from Sangon Biotech (Shanghai) Co., Ltd. The basic medium contained (g $L^{-1}$): $NH_4Cl$ 0.2, $Na_2SO_4$ 0.5, $KH_2PO_4$ 2.66 and yeast extract 3. The complex activator comprises epigallocatechin gallate at a mass concentration of 2.5 g/L, theanine at a mass concentration of 2.5 g/L, ascorbic acid at a mass concentration of 6.5 g/L, $H_3BO_3$ at a mass concentration of 6.5 g/L, $FeCl_3$ mass concentration of 4.5 g/L, and $MgCl_2$ mass concentration of 0.05 g/L.

All the above culture media were adjusted to pH 6.0 and sterilized with a high-pressure sterilizer at 121℃ and 0.10 MPa for 20 minutes.

In this study, the original microbial source used for screening the functional microbiome was activated sludge from a simulated hydrolysis acidification tank in the laboratory. The activated sludge came from the reflux sludge of the second sedimentation tank of Songdong Wastewater Treatment Plant in Songjiang District, Shanghai. The initial sludge concentration was 4560 mg/L, and the sedimentation performance was good.

# 1.2. Decolorization

Took 10 mL of DDMZI/DDMY1 that had been cultured for 48 hours with a 10% (V/V) inoculation amount and added it to a conical flask containing 90 mL of fresh YE medium. Added RB5/RBBR to achieve a final concentration of 100 mg/L. Incubated at a constant temperature of 37℃. After a certain period of cultivation, took 2 mL of decolorization solution and fully contacted it with oxygen. Centrifuged at 6200×g for 10 minutes and observed the color changes before and after contact with oxygen. Using YE culture medium as a blank, measured the absorbance value of the supernatant at the characteristic wavelength of 597 nm. Calculated the decolorization ratio according to formula (1), and repeated the process 3 times.

$$A_d = \frac{(A_0 - A_t)}{A_0} \times 100\%$$

1

In the formula, $A_d$ is the decolorization ratio at the measured time; $A_0$ is the characteristic peak value of the dye solution at time 0; $A_t$ is the characteristic peak measured at time t.

# 1.3. Domestication of functional microbiome

Took 10 mL of fresh activated sludge from the anoxic tank of the well that was running a simulated dye wastewater hydrolysis acidification tank in that experiment and added it to a 250 mL conical flask containing 90 mL of basic culture medium. Incubated it in a constant temperature incubator at 37 ℃ for 48 h. At the same time, the microbial density in the culture medium was measured using a blood cell

counting plate. When the microbial density measured by the blood cell counting plate was greater than $10^8$ cells/mL and the OD600 was around 1.5, transfer the microbial solution at a rate of 10% (V/V) into domestication medium (domestication medium: anhydrous sodium sulfate 0.5 g/L, ammonium chloride 0.2 g/L, potassium dihydrogen phosphate 2.66 g/L, yeast extract 3 g/L, RBBR ranging from 10 to 100 mg/L). When domesticating, the dye concentration started from 10 mg/L of Reactive Brilliant Blue 19 and was incubated at a constant temperature of 37 ℃ for 48 h to determine the decolorization ratio. When the decolorization ratio reached 80% or more, it was transferred to a domestication medium with a higher dye concentration. When the decolorization ratio of the mixed microbial community on 100 mg/L of active brilliant blue 19 reached over 80% after 48 hours, domestication was completed, and it was considered that a functional microbiome with high efficiency in degrading high concentrations of active brilliant blue 19 had been screened and named DDMY1. DDMY2 was co-cultured and domesticated using the domestication medium containing tea leaf residue at a mass concentration of 3 g/L.

In the later stage, to study the removal effect of functional microbiome on azo dyes, RB5 was used to domesticate the functional microbiome DDMY1. The domestication medium contained (g $L^{-1}$): $NH_4Cl$ 0.2, $Na_2SO_4$ 0.5, $KH_2PO_4$ 2.66, yeast extract 3 and RB5 ranging from 10 to 100 mg/L. Domestication had been completed, and it was believed that a functional microbiome with high efficiency in degrading high concentrations of RB5 had been screened and named DDMZ1.

## 1.4. Effects of different electron donors and acceptors on the community structure of functional microbiome

In this study, different electron donors and electron acceptors were selected to investigate the changes in the community structure of DDMZ1 and its keystone species. Four groups were selected as different electron donors: inorganic salts (MN), fructose (FRU), yeast extract (YE), and yeast extract + fructose (YE + FRU). Five different structural dyes were selected as different types of electron acceptors: AO7, RB5, CBE, RBBR, and MG. AO7 is a monoazo dye, RB5 is a diazo dye, CBE is a triazo dye, MG is a triphenylmethane dye, and RBBR is an anthraquinone dye. In addition, four different concentrations of azo dye RB5 (0 mg/L, 100 mg/L, 200 mg/L, and 400 mg/L) were selected as different concentrations of dye electron acceptors.

## 1.5. DNA extraction, PCR amplification and sequencing with Illumina MiSeq

The detailed experimental operation was in accordance with manufacturer’s instructions. Total DNA of all samples were extracted by E.Z.N.A.® Soil DNA Kit (Omega Bio-tek, Norcross, GA, U.S.) according to manufacturer’s protocols. Using extracted DNA as a template, primers 515F (5 'GTGCCAGCMGCGG-3') and 907R (5'-CCGTCAATTCMTTTRAGTTT-3') were used to amplify the V4 and V5 regions of 16S rDNA. The Illumina MiSeq sequencing method was employed to do this investigation. After sequencing, raw fastq files were demultiplexed and quality-filtered using Quantitative Insights into Microbial Ecology (QIIME). In order to further improve the quality of analysis results, before conducting bioinformatics

analysis, the raw data obtained must be filtered and processed to obtain an optimized sequence. After sequencing, in order to reduce the inaccuracy of sequencing results caused by different sequences, it is necessary to ensure that the same number of sequences are used when comparing microbial communities between different samples. Using UPARSE (version 7.1 http://drive5.com/uparse/)Assign these sequences as classification units OTUs (97% similarity).

## 1.6. Statistical analysis

Based on the OTU clustering analysis results, the Mothur software package was used to analyze the diversity indices and dilution curves of Chao, Ace, Simpson, Coverage, and Shannon.Based on taxonomic information, using RDP software package (http://rdp.cme.msu.edu/)Perform phylogenetic analysis on sequences at the taxonomic level. Based on the different microbial community compositions of different samples, hierarchical aggregation, principal co-ordinates analysis (PCoA), fold change, Abundance Circos plot and Nonmetric Multidimensional Scalin (NMDS), were performed on each sample using the R software package. Besides, to examine relationship among microbial community, the co-occurrence network was constructed as the previous study of Peng et al[15]. In order to identify key species in the microbial association network, ZIPI analysis was performed on the samples. Node attributes can be categorized into four types based on the topological characteristics of the node, including: Module hubs (module centers, nodes with high connectivity within the module, Zi > 2.5 and Pi < 0.62), Connectors (connection nodes, nodes with high connectivity between the two modules, Zi < 2.5 and Pi > 0.62), Network hubs (network centers, nodes with high connectivity throughout the network, Zi > 2.5 and Pi > 0.62), and Peripherals (peripheral nodes, nodes that do not have high connectivity within and between modules, Zi < 2.5 and Pi < 0.62). The remaining 3 types of nodes other than Peripherals are usually categorized as critical nodes[16]. An analytical framework was used to quantify the relative roles of deterministic and stochastic processes based on the null model method and phylogenetic data.βNTI and RCbray can be classified into different regions, including Heterogeneous Selection(βNTI > 2), Homogeneous Selection(βNTI < -2), Dispersal Limitation(|β-NTI| < 2 and RCbray > 0.95), Homogenizing Dispersal(|β-NTI| < 2 and RCbray < − 0.95), Undominated(|β- NTI| < 2 and |RCbray| < 0.95). Meanwhile, the R package of Tax4Fun2 was utilized to rapidly predict the functional profiles and functional redundancy of prokaryotes based on 16S rRNA gene sequences, and to analyze the functional changes of microbiome over the decade.

# 2. Results and discussion

## 2.1. Decoloration ratio

The functional microbiome DDMY1, which was capable of efficiently decolorizing Reactive Brilliant Blue 19, was finally obtained after being screened and domesticated through 10 anthraquinone dye concentration gradients over a period of 1 year and approximately 150 generations, utilizing gradient concentration pressure domestication. As shown in Fig. 1 (a), the 48 h decolorization ratio of 100 mg/L RBBR by functional microbiome DDMY1 was able to reach more than 98% in 2015. Domestication of

DDMY1 with azo dyes using RB5 in March 2016 resulted in DDMZ1, a functional microbiome capable of efficiently degrading azo dyes. After one year of domestication DDMZ1 was able to achieve 95% decolorization ratio of 100 mg/L azo dye RB5(Fig. 1 (b)). Overall, the two functional microbiomes maintained a better decolorization ratio effect in the long term. It is presumed that the long-term stable culture environment contributed to the stability of the microbiome structure.

According to Fig. 1(c), it was found (this part of the data has been published [17]) that the decolorization of DDMY2 was better than that of DDMY1 when treating 200 mg/L of RBBR. DDMY2 differed from DDMY1 in that the former had been domesticated together with the addition of tea dregs during the long-term domestication process, so it was presumed that the difference in decolorization ratios was due to the activation of tea dregs. It was also seen that the complex activator had a significant enhancement on the decolorization ability of the functional microbiome. Figure 1(d) demonstrated the changes in decolorization ratio of functional microbiome DDMZ1 treating different structural types of dyes. It was seen that in azo dyes, the decolorization ability of DDMZ1 was enhanced with the reduction of azo groups. DDMZ1 showed strong decolorization ability in the late stage of decolorization of triphenylmethane dyes, while the decolorization ability of anthraquinone dyes was slightly lower than that of the other two types of dyes. Overall, the functional microbiome DDMZ1 showed good degradation of different types of dyes. Figure 1(e) showed the ability of functional microbiome to decolorize the azo dye RB5 by treating different concentrations. It could be seen that the functional microbiome had a high decolorization ratio of 72.1% at 72 h in the presence of a high concentration of dye at 400 mg/L, demonstrating a high decolorization capacity. At the same time, it was obvious that the decolorization ratio decreased with increasing dye concentration. Figure 1(f) showed the effect of the presence of different electron donors on the decolorization ability of functional microbiome. According to the decolorization ratio, it was seen that YE + FRU>YE > FRU>MN, and the YE + FRU group was the most effective, with a decolorization ratio of up to 98.5%.

In summary, the three groups of autonomously domesticated natural microbiomes exhibited significant functionality in the biological treatment of dye wastewater. Additionally, variations in environmental factors during the domestication and application processes had a crucial impact on the expression of the microbiomes' functionality.

## 2.2. Studies on the evolution of functional microbiome during the domestication stage

Figure 2(a) showed a hierarchical clustering tree diagram of the microbiome of DDMY1 during domestication and use, indicating the evolutionary relationship of functional microbiome during domestication. Sequences of samples belonging to the same branching class had a similar evolutionary relationship, which indicated that the functional microbiome evolved over time as domestication and application progressed. During the one-year period of functional microbiome application following domestication, the microbiome underwent significant evolution and had already diverged into a distinct branch from its original domestication stage. Figure 2(b) showed the analysis of βNTI/RCbray

community structure of DDMY1 during domestication and application. Firstly, the two-year process of domestication and application of DDMY1 was dominated by stochastic evolution with genetic drift. Some of the quantitative data had RCbray values greater than 0.95, suggesting that the functional microbiome also underwent diffusion-restricted stochastic evolution without homogeneous diffusion, and presumably involved fewer microbial community interactions within the functional microbiome. Functional microbiome underwent a small amount of deterministic evolution (201501–201503, 201503–201506), suggesting that changes in its community structure were not randomly expected, but rather that physico-chemical conditions during domestication had a driving influence on the community composition.

Alpha diversity is a reflection of the abundance and diversity of microbiome. As can be seen in Table 1, the coverage data indicated that the results were generally indicative of the true state of the microorganisms in the samples. In the pre-domestication period of 0–6 months, Shannon's index was greater with longer domestication time, and Simpson's index, indicating that functional microbiome increased in microbial diversity in the pre-domestication period with increasing domestication time. The data based on the the Ace and Chao indices showed that the species abundance of functional microbiome increased in the pre-domestication period with the increase in the duration of domestication. In the later stages of domestication, the diversity of functional microbiome declined and the abundance increased with increasing domestication time. Overall, the diversity of the microbiome decreased in the late stage of domestication compared to the early stage, and the abundance showed a trend of increasing and then decreasing with the time of domestication. Maximum abundance was reached at 3 months of domestication. During the application phase of the functional microbiome, an increase in microbial diversity was observed, accompanied by a decrease in the abundance of microbial. It is hypothesized that anthropogenic activities, such as domestication and application, significantly influenced microbiome evolution.

Table 1
Alpha diversity during DDMY1 domestication and application

| Sample | Phase | Sobs | Shannon | Simpson | Ace | Chao | Coverage |
|---|---|---|---|---|---|---|---|
| 0M | Pre-domestication | 9 | 0.670559 | 0.573068 | 9.373779 | 9 | 0.99997 |
| 3M | | 15 | 0.866241 | 0.481677 | 15 | 15 | 1 |
| 6M | | 20 | 0.888257 | 0.469446 | 22.722886 | 21 | 0.999918 |
| 10M | Late stage of domestication | 10 | 0.885563 | 0.472989 | 0 | 9.333333 | 0.99993 |
| 11M | | 9 | 0.872402 | 0.565624 | 12.886969 | 11 | 0.999942 |
| 20M | Application phase | 18 | 1.102678 | 0.499872 | 18.474966 | 18 | 0.999971 |
| 24M | | 13 | 1.457159 | 0.252125 | 14.680891 | 13.5 | 0.999934 |

The results of the modularity analysis showed that the DDMY1 association network was mainly composed of two association modes such as intra-module and inter-module interactions. *Lachnoclostridium* (OTU14), *Lachnoclostridium_5* (OTU15) and *Tyzzerella* (OTU16) constituted Module 1. Other microorganisms constituted one Module 2. According to the Network correlation network analysis diagram in Fig. 3, it could be seen that the DDMY1 community structure was predominantly intra-module 2 interactions. *Clostridium_sensu_stricto_12* had the highest value in the center of all nodes and was the most important in the network structure. *Clostridium_sensu_stricto_12* was recognized as a key microorganism for acetic acid production [18], which played an important function in the treatment of DDMY1 dye wastewater. It was worth noting that microorganisms were clearly positively correlated with each other in the community structure, with only *Burkholderia* (OTU10) showing negative correlation with both *unclassified_o_Pseudomonadales* (OTU12) and *Enterococcus* (OTU13). According to Abilaji et al.[19] macro genomic results showed that *Enterococcus* (OTU13) was involved in the biodegradation of textile wastewater. The study of Wang et al.[20] found that *Enterococcus* (OTU13) was able to achieve 81.95% decolorization of 50 mg/L RB5. Zhang et al.[21] also found that *Burkholderia* (OTU10) had a good decolorization ratio for azo dyes, and the decolorization ratio for RB5 at 200 mg/L could reach 76%. The functionality of *unclassified_o_Pseudomonadales* (OTU12) for dye degradation had been reported relatively little. Both *Burkholderia* (OTU10) and *Enterococcus* (OTU13) possess dye degradation functions in DDMY1, and it was hypothesized that the negative correlation presented by the two inhibits the functionality of DDMY1. During the evolution of microbial communities, while continually enhancing functionality, there emerged community relationships that inhibited the expression of that functionality.

## 2.3. Effects of complex activators on the evolution of functional microbiome

PcoA analyses, NMDS analyses, and correlation analyses are able to assess the effects of different domestication processes on the evolution of functional microbiome communities. Network correlation network analysis enables the study of the co-existence of community species in the presence of different domestication processes. According to the PcoA analysis depicted in Fig. 4(a), it could be observed that DDMY1, which had been domesticated exclusively by RBBR, exhibited a certain degree of similarity in the evolution of its microbiological population after 6 months of domestication, yet it remained within the same quadrant. However, after the addition of the complex activator, the relative coordinate points of the two groups of samples (D1A vs. 6D1A) were already in different quadrants compared to D1 and 6D1. And D1A was not in the same quadrant as its sample 6D1A obtained after 6 months of domestication, and the evolution of the microbiome was obvious. While for the microbiome DDMY2, which had been co-domesticated by RBBR and tea residue, the effect produced by the composite activator was less pronounced, remaining largely within the same quadrant, the evolution of the microbiome was not evident. This could also be clearly discerned through the NMDS analysis (Fig. 4(b)). For DDMY2, the effects produced by prolonged domestication were likely to be greater than the effects of the complex activator.According to the correlation clustering analysis in Fig. 4 (c), it could be seen that sample group D1 (D1A and 6D1A (X6D1A)) with the addition of the composite activator

belonged to the same cluster as group D2 domesticated by tea residue. In summary, it was hypothesized that because the composite activator better simulated the activation function of tea dregs for the microbiome, both of them provided the same culture environment to promote the deterministic evolution of functional microbiome.

According to the network correlation analysis of DDMY1 in Fig. 4 (d), it could be seen that the microbiome could be categorized into three plates, and both intra- and inter-plate interactions played very important roles. Plate I and Plate II were in a many-to-many mutualistic relationship, and *norank_f__PHOS-HE36* (OTU16) connected the two plates. *Norank_f__PHOS-HE36* (OTU16) was also the most highly correlated microorganism in the microbiome and was found to be mostly used in metal metabolism as well as in reaction systems such as denitrification [22, 23]. In Plate I, *Enterococcus* (OTU17) showed negative correlation with all microorganisms in Plate I. *Enterococcus* (OTU17) had been documented by many to possess dye-degrading functions[24–26], and was hypothesized to play an important role in the functional microbiome DDMY1. Li et al.[27] found that the relative abundance of *norank_o__JG30-KF-CM45* (OTU14) was negatively correlated with $NH_3$. The reduction of azo dyes by *Enterococcus* (OTU17) under parthenogenetic anaerobic conditions might have produced a certain amount of ammonia, leading to a negative correlation.

PcoA analysis, NMDS analysis, and correlation analysis revealed that the effect of complex activators on the deterministic evolution of functional microbiome was more pronounced compared to long-term domestication.

Therefore, the study used Fold change to reflect species characterization data with up- or down-regulation of abundance (Fig. 4(e)) as a way to further analyze the effect of complex activators on the evolution of functional microbiome. First for DDMZ1, the addition of the complex activator significantly increased the abundance of *Pseudomonas* and decreased the abundance of *Lachnoclostridium*. *Pseudomonas* had a better degradation effect [28], which is also corroborated by the fact that the addition of activators contributed to the functional microbiome decolorization ratio. Huang et al.[29] also showed that the addition of tea polyphenols contained in the complex activator resulted in a decrease in *Lachnoclostridium* abundance. Zeng et al[30]. believe that *Burkholderia-Paraburkholderia* was negatively correlated with epigallocatechin gallate. The results of the decrease in the abundance of *Burkholderia-Paraburkholderia*, which were observed due to the addition of activators, were consistent with their previous findings. For DDMY2, the effect of activators was smaller compared to DDMY1, with the largest increase in the abundance of *Azoarcus* and a significant decrease in the abundance of *norank_f__Veillonellaceae*. Polysaccharides from Fuzhuan brick tea (FBTPS), one of most important bioactive components in tea. Chen et al.[31] found that the addition of FBTPS induced a significant increase in the abundance of *norank_f__Veillonellaceae*. DDMY2 had been domesticated with tea leaf residue, which contains FBTPS but not in the added complex activator, so it was hypothesized that the absence of this substance had led to a decrease in the abundance of *norank_f__Veillonellaceae*.

DDMY1 and DDMY2 were subjected to activator addition and six-month domestication to study their evolutionary process, and the results of βNTI/RCbray community structure analysis were shown in Fig. 4 (f). As can be seen, all of the evolution of the two groups of colonies was stochastic. Genetic drift was dominant, with a small amount of diffusion limitation. The functional microbiome DDMY1 after 6 months of domestication showed a clear diffusion limitation between the other three groups. It was hypothesized that diffusion limitation occurred mainly due to spatial as well as temporal separation and the inability of microorganisms to interact between samples, resulting in ecological drift over time.

## 2.4. Effects of changing environmental factors on the evolution of functional microbiome

### 2.4.1. Different structural types of dye electron acceptors

Functional microbiome DDMZ1 had a better effect on the treatment of dyeing wastewater, and different structural types of dyes affected the community structure and the evolution of the microbiome. Figure 5(I) represented the graph of structural changes of functional microbiome under the influence of different structural types of dye electron acceptors. The effect of different types of dyes on the structure of microbiome was evident, with significant differences in community structure in the presence of azo dyes, triphenylmethane and anthraquinone dyes. DDMZ1 was domesticated from the azo dye RB5. The community structure of the double azo dye (RB5) and triple azo dye (CBE) groups was similar to that of the functional microbiome DDMZ1 in the absence of the dye, and differed somewhat from that in the presence of the single azo dye (AO7). The larger proportion (37.62%) of *Enterococcus* (OTU12) was the main reason for the difference in community structure between those affected by single azo dyes and those affected by other azo dyes. A number of studies had shown that *Enterococcus* (OTU12) had been applied to dye biodegradation because of its better functionality[24, 25]. *Enterococcus* (OTU12) was hypothesized to be capable of degrading dyes with relatively simple structures and to had relatively low tolerance for more complex and toxic azo dyes. *Pseudomonas* (OTU19) showed a large percentage (87.58%) in anthraquinone dyes, which was hypothesized to have a better removal ability for anthraquinone dyes, which was in agreement with the findings of Wang et al.[32]. *Stenotrophomonas* (OTU11, 26.80%), *Escherichia-Shigella* (OTU18, 38.36%) and *Pseudomonas* (OTU19, 21.51%) were more predominant in the MG group, which differed considerably from the community structure under the influence of the azo dye group. The structure of the community affected by triphenylmethane dyes was clearly more complex compared to azo dyes as well as anthraquinone dyes.

### 2.4.2. Different concentrations of dye electron acceptors

The effects of different concentrations of azo dye RB5 on the community structure of functional microbiome were shown in Fig. 5(II). The composition of the microbiome was more complex in the absence of dye presence, while the community structure was gradually simplified as the dye concentration increased. *Stenotrophomonas* (OTU5) had a large occupancy at low concentrations, but no significant occupancy was seen at the high concentration of 400 mg/LRB5, hence it was hypothesized

that the high toxicity of the dye at its high concentration had an effect on its activity. The abundance of *Burkholderia-Paraburkholderia* (OTU6) was higher at 400 mg/LRB5 (58.37%) than 200 mg/LRB5 (28.79%). It was hypothesized that *Burkholderia-Paraburkholderia* (OTU6) played an important role in the decolorization of dyes at high concentrations by functional microbiome.

## 2.4.3. Different types of electron donor

According to Fig. 5(III-a), it could be seen that the results of functional microbiome changed significantly in the presence of different electron donors. The microbiome of the YE and MN groups were more similar. It was hypothesized that the community structure had stabilized because the domestication medium for the functional microbiome contains YE, and that the microbiome changes less when YE was not added. *Lactococcus* (OTU13) had the largest percentage in YE (58.42%) vs. MN (71.72%), which was not a major functional microorganism as presumed based on the decolorization ratios of different electron donors. When the electron donor was FRU group, the microbiome was more complex, in which *Escherichia-Shigella* (OTU18) dominated. Tacas et al.[33] found that *Escherichia-Shigella* (OTU18) had a better extracellular electron transfer capacity, which favors dye degradation. When YE was compounded with FRU as an electron donor, the community structure was similar to that of the YE group, and it was hypothesized that YE group had a greater effect on the microbiome compared to FRU group.

Figure 5(III-b) showed the ZIPI analysis for the effect of different donors on microbiome evolution, and the remaining three types of nodes except Peripherals were categorized as key nodes. *Chroococcidiopsis_SAG_2023* (OTU1, (0.6667, 0.866)) and *Burkholderia-Caballeronia-Paraburkholderia* (OTU3, (0.625, 1.1547) were all of the Connectors type, nodes with a high degree of connectivity between the two modules, and could be fully categorized as critical nodes. Combined with the Circos plot and decolorization ratio, *Burkholderia-Caballeronia-Paraburkholderia* (OTU3) had the largest percentage in the YE + FRU group, which had the highest decolorization ratio, and thus it was hypothesized that *Burkholderia-Caballeronia- Paraburkholderia* (OTU3) played an important functional role in the microbiome.

In summary, environmental factors had a significant impact on community structure, and changes in community structure also affected the evolution of the microbiome. YE group electron donors had the greatest influence on the microbiome. Burkholderia-Caballeronia-Paraburkholderia was the key functional microorganisms within the microbiome. The conclusions drawn can be leveraged to strategically guide the evolution of the microbiome.

# 2.5. A decade long application of functional microbiome evolutionary studies

## 2.5.1. Changes in microbiome diversity

Table 2 showed the Alpha diversity data during the decade of DDMZ1 domestication and application. The Coverages data indicate that all measurements were reliable. Simpson's index could be used to

characterize the concentration of community composition, with higher values indicating higher concentration and lower diversity. According to Table 2, it could be seen that Shannon index gradually increased and Simpson index gradually decreased over the five years from 2015–2019, and the diversity of functional microbiome gradually increased. The diversity of functional microbiome gradually decreased over the four years from 2021–2024. The overall trend of functional microbiome diversity over the decade was first increasing and then decreasing. It was hypothesized that in the initial stage, the increase in diversity might be due to the gradual diversification of the microbiome through adaptive evolution to new habitats under different environmental conditions. However, over time, long periods of unchanging culture environments might lead to the dominance of certain strains, which might result in a decrease in diversity.

Table 2
Alpha diversity during a decade of DDMZ1 domestication and application

| Sample | Sobs | Shannon | Simpson | Ace | Chao | Coverage |
|---|---|---|---|---|---|---|
| 2015 | 13 | 0.797284 | 0.484319 | 13.460219 | 13 | 0.999973 |
| 2016 | 9 | 1.276632 | 0.326386 | 9 | 9 | 1 |
| 2018 | 22 | 1.603299 | 0.330105 | 22 | 22 | 1 |
| 2019 | 13 | 1.897976 | 0.17909 | 13 | 13 | 1 |
| 2021 | 14 | 1.769325 | 0.223585 | 14 | 14 | 0.99998 |
| 2022 | 11 | 1.380235 | 0.39922 | 11 | 11 | 1 |
| 2024 | 7 | 0.917385 | 0.448764 | 7.424427 | 7 | 0.999982 |

## 2.5.2. Evolution of functional microbiome

Figure 6(a) showed the community structure composition and changes of functional microbiome DDMZ1 during the ten-year domestication and application process. It was obvious that the microbes in the functional microbiome mainly belong to two phyla, *Firmicutes* and *Proteobacteria*. *Burkholderia* and *unclassified_f__Enterobacteriaceae* dominated the initial microbiome, but the abundance of both gradually decreased during microbiome domestication and prolonged application. *Klebsiella*, *Escherichia-Shigella* and *Stenotrophomonas* gradually dominated. Many studies had also shown that the three microorganisms mentioned above could play an important role in dye degradation[33–35]. Figure 6(b) demonstrated the results of calculating the stochastic and deterministic evolution of functional microbiome based on βNTI/RCbray, and it was clearly visible that the evolution of functional microbiome over the decade had shown significant deterministic evolution. The quantified interannual variation was mainly distributed in the βNTI > 2 range, with dispersed genetic distances for OTUs, showing that the interannual variation of the microbiome was mainly dominated by biological interactions. Whereas annual variation was mainly in the βNTI<-2 range, the genetic distance of OTUs converged and was dominated by environmental selection. Deterministic evolution helps to maintain and optimize the

functional microbiome[36]. Functional microbiome was screened for microbial species that were adapted to specific environments through a deterministic evolutionary process under specific environmental conditions. These microorganisms worked together to perform specific functions through interaction and coordination. The microbiome had maintained deterministic evolution, presumably due to the long-term consistency of the culture environment of the microbiome over a ten-year period.

Figure 6(c) illustrated the key species in the microbial association network of functional microbiome over the decade. *Burkholderia* (0.625, 1.1547) with Pi > 0.62, the study concluded that nodes with high connectivity between the two modules were keystone species for functional microbiome. However, changes in community structure over the decade showed that the key species, *Burkholderia*, decreased as a percentage of the microbiome with microbiome application. Several studies had demonstrated the strong degradation capacity of the key species *Burkholderia* in dyeing wastewater[37, 38]. Therefore, in order to improve the dye degradation ability of the microbiome, subsequent artificial regulation of their abundance is considered necessary.

## 2.6. Prediction of functional microbiome

Rapid prediction of functional profiles of microbiome from 16SrRNA gene sequences contributes to a deeper understanding of the functional properties of microbiome in specific environments or conditions. From Fig. 7, it could be seen that the main functions of DDMZ1 were Carbohydrate metabolism and Lipid metabolism. Both are basic and important functions in microbial communities. They provide energy and building materials for microorganisms. This function of Xenobiotics biodegradation and metabolism is important for the maintenance of ecosystems. Overall, the expression of Xenobiotics biodegradation and metabolism function gradually increased during the decade, which showed that the functional microbiome DDMZ1 was able to show stronger functionality after long-term domestication and application. It was also evident that the functional expression of DDMZ1 in the microbiome remained essentially stable over the ten-year period, which corroborates the deterministic evolution derived from 2.5.2 Evolution of functional microbiome.

## 3. Conclusions

The functional microbiome had good decolorization ability for dye wastewater. The changes of environmental factors had a great influence on the community structure of functional microbiome. Under the influence of short-term environmental factors, the microbiome was dominated by stochastic evolution. However, long-term tracking and monitoring of the functional microbiome revealed that the functional microbiome was basically dominated by deterministic evolution during 10 years of domestication and application. This indicates that the functional microbiome had better stability as well as adaptability when the culture conditions were kept constant, which was conducive to maintaining and optimizing the function of the microbiome. And the interannual evolution of microbiome was mainly influenced by biological interactions, while the intra-annual evolutionary process was mainly dominated

by environmental selection. At the same time the functional microbiome expression remained stable and the function of Xenobiotics biodegradation and metabolism expression gradually increased.

# Declarations

**Declaration of interests**

 The authors declare that they have no known competing financial interests or personal relationships that could have appeared to influence the work reported in this paper.

 The authors declare the following financial interests/personal relationships which may be considered as potential competing interests:

Xin Liu：Writing – original draft, Formal analysis, Conceptualization, Investigation

Yiting Qin: Writing – original draft, Formal analysis, Software, Methodology, Visualization

Jiajie Liu: Resources, Project administration

Wanting Li: Resources, Software, Supervision

Xinyi Guo: Software, Validation, Visualization

Na Liu: Project administration, Funding acquisition

Qingyun Zhang: Project administration, Funding acquisition

Xuehui Xie: Writing – review and editing, Validation, Project administration, Funding acquisition

Ye Chen: Writing – review and editing, Methodology, Resources, Funding acquisition

# Author Contribution

Xin Liu：Writing – original draft, Formal analysis, Conceptualization, InvestigationYiting Qin: Writing – original draft, Formal analysis, Software, Methodology, VisualizationJiajie Liu: Resources, Project administrationWanting Li: Resources, Software, SupervisionXinyi Guo: Software, Validation, VisualizationNa Liu: Project administration, Funding acquisitionQingyun Zhang: Project administration, Funding acquisitionXuehui Xie: Writing – review and editing, Validation, Project administration, Funding acquisitionYe Chen: Writing – review and editing, Methodology, Resources, Funding acquisition

# Acknowledgement

The authors acknowledge the Fundamental Research Funds for the Central Universities, China (grant numbers 2232024A-02□2232022G-01). The Innovation Team for Reducing Pollution and Carbon Emissions in the Agricultural Ecological Environment of Northern Anhui (grant number 2024TD02). The scientific research program of Anhui Provincial Education Department (grant number 2025AHGXZK60086), the Innovation and Entrepreneurship Training Program for College Students (grant number 202110363068).

# Data Availability

All data supporting the findings of this study are available within the paper and its Supplementary Information.

## References

1. Barbelli-Lopez, M.S., M.P. Peralta, L. Levin, et al., *Effect of co-cultivation of white and brown rot species on basidiome production, lignocelluloytic enzyme activity and dye decolourisation*. Bioresource Technology, 2024. 395: p. 130397.
2. Zhao, H.-Q., N. Hou, Y.-R. Wang, et al., *Carbon nanotubes mediated chemical and biological decolorization of azo dye: Understanding the structure-activity relationship*. Environmental Research, 2022. 210: p. 112897.
3. Song, Y., L. Wang, X. Qiang, et al., *An overview of biological mechanisms and strategies for treating wastewater from printing and dyeing processes*. Journal of Water Process Engineering, 2023. 55: p. 104242.
4. Xu, H., B. Yang, Y. Liu, et al., *Recent advances in anaerobic biological processes for textile printing and dyeing wastewater treatment: a mini-review*. World Journal of Microbiology and Biotechnology, 2018. 34: p. 1–9.
5. Zhu, Y., J. Xu, X. Cao, et al., *Characterization of functional microbial communities involved in different transformation stages in a full-scale printing and dyeing wastewater treatment plant*. Biochemical engineering journal, 2018. 137: p. 162–171.
6. Ni, H., M. Arslan, J. Wei, et al., *Treatment of printing and dyeing wastewater in biological contact oxidation reactors comprising basalt fibers and combination fillers as bio-carriers: Elucidation of bacterial communities and underlying mechanisms*. Science of The Total Environment, 2021. 785: p. 147272.
7. Sengupta, A., T.H. Volkmann, R.E. Danczak, et al., *Contrasting community assembly forces drive microbial structural and potential functional responses to precipitation in an incipient soil system*. Frontiers in Microbiology, 2021. 12: p. 754698.
8. Corno, G., Y. Yang, E.M. Eckert, et al., *Effluents of wastewater treatment plants promote the rapid stabilization of the antibiotic resistome in receiving freshwater bodies*. Water research, 2019. 158: p. 72–81.

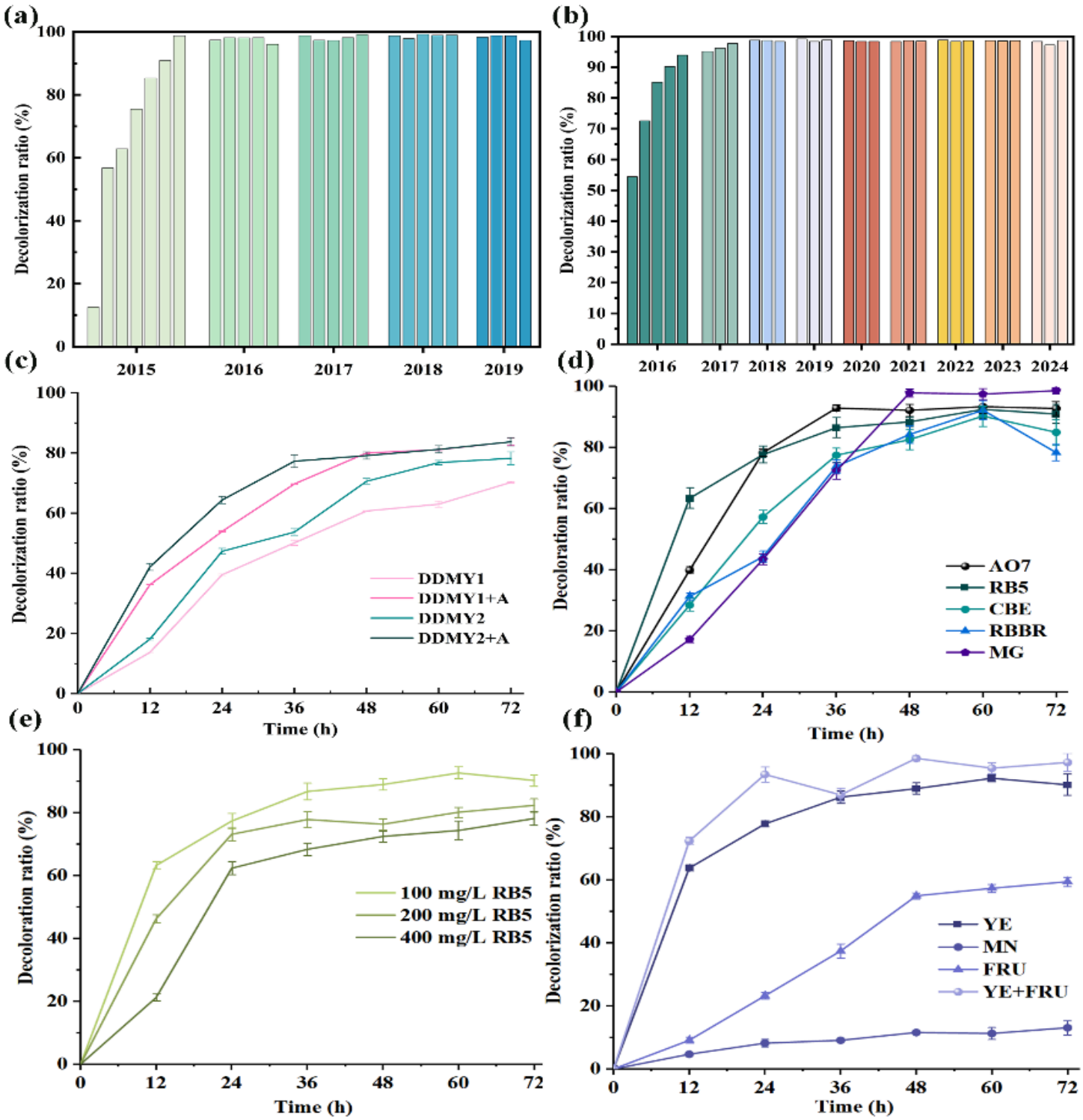
9. Liu, J., Z. Meng, X. Liu, et al., *Microbial assembly, interaction, functioning, activity and diversification: a review derived from community compositional data*. Marine Life Science & Technology, 2019. 1: p. 112–128.
10. Yun, Y., Z. Gui, J. Xie, et al., *Stochastic assembly process dominates bacterial succession during a long-term microbial enhanced oil recovery*. Science of The Total Environment, 2021. 790: p. 148203.
11. Campos, P.M., L.L. Schreier, M. Proszkowiec-Weglarz, et al., *Cecal microbiota composition differs under normal and high ambient temperatures in genetically distinct chicken lines*. Scientific Reports, 2023. 13(1): p. 16037.
12. Irl, S.D., A. Obermeier, C. Beierkuhnlein, et al., *Climate controls plant life-form patterns on a high-elevation oceanic island*. Journal of Biogeography, 2020. 47(10): p. 2261–2273.
13. Zhou, J. and D. Ning, *Stochastic community assembly: does it matter in microbial ecology?* Microbiology and molecular biology reviews, 2017. 81(4): p. 10.1128/mmbr. 00002–17.
14. Zhang, J., A. Hu, Y. Sun, et al., *Dispersal limitation expands the diversity of coral microbiome metacommunity in the South China Sea*. Frontiers in Marine Science, 2021. 8: p. 658708.
15. Peng, Q., H. Zheng, H. Yu, et al., *Environmental factors drive the succession of microbial community structure during wheat Qu fermentation*. Food Bioscience, 2023. 56: p. 103169.
16. Putman, L.I., M.C. Sabuda, W.J. Brazelton, et al., *Microbial communities in a serpentinizing aquifer are assembled through strong concurrent dispersal limitation and selection*. Msystems, 2021. 6(5): p. 10.1128/msystems. 00300 – 21.
17. Wang Yiqin, Xie Xuehui, Zheng Xiulin, et al., *Promotional effect of compound activators on the degradation of activated brilliant blue by mixed microbiome and biodegradation mechanism*. Journal of Donghua University (Natural Science Edition), 2021. 47(2).
18. Chen, R., X. Zhou, L. Huang, et al., *Effects of yeast inoculation methods on caproic acid production and microbial community during anaerobic fermentation of Chinese cabbage waste*. Journal of Environmental Management, 2024. 356: p. 120632.
19. Abilaji, S., K. Sathishkumar, J. Narenkumar, et al., *Sequential photo electro oxidation and biodegradation of textile effluent: Elucidation of degradation mechanism and bacterial diversity*. Chemosphere, 2023. 331: p. 138816.
20. Wang, R., H. Li, Y. Liu, et al., *Efficient removal of azo dyes by Enterococcus faecalis R1107 and its application in simulated textile effluent treatment*. Ecotoxicology and Environmental Safety, 2022. 238: p. 113577.
21. Zhang, Q., X. Xie, Y. Liu, et al., *Sugar sources as Co-substrates promoting the degradation of refractory dye: A comparative study*. Ecotoxicology and Environmental Safety, 2019. 184: p. 109613.
22. Xin, X., B. Li, X. Liu, et al., *Starting-up performances and microbial community shifts in the coupling process (SAPD-A) with sulfide autotrophic partial denitrification (SAPD) and anammox treating nitrate and ammonium contained wastewater*. Journal of Environmental Management, 2023. 331: p. 117298.

23. Tong, T., J. Tong, K. Xue, et al., *Microbial community structure and functional prediction in five full-scale industrial park wastewater treatment plants*. Science of The Total Environment, 2023. 904: p. 166529.
24. Song, P., W. Feng, H. Shi, et al., *Efficient Decolorization of Water and Oil-Soluble Azo Dyes by Enterococcus avium Treated with HP-β-CD*. Pakistan Journal of Zoology, 2019. 51(2): p. 675–680.
25. Nazari, N. and F.J. Kashi, *A novel combination of immobilized Enterococcus casseliflavus sp. nov. with silver nanoparticles into a reusable matrix of Ca-Alg beads as a new strategy for biotreatment of Disperse Blue 183: Insights into metabolic characterization, biotoxicity, and mutagenic properties*. Journal of Environmental Management, 2023. 325: p. 116578.
26. Rathod, J., S. Pandey, K. Mahadik, et al., *Homologous overexpression of azoreductase (azoA) in Enterococcus sp. L2 moderated growth and azo dye decolorization while gaining an oxidative and heavy metal stress resistance: A trade-off*. Environmental Technology & Innovation, 2022. 27: p. 102531.
27. Li, C., G. Pan, X. Wang, et al., *The effects of non-metallic organic tanning agents on the microbial community structure in wastewater*. Journal of cleaner production, 2021. 279: p. 123553.
28. Garg, N., A. Garg, and S. Mukherji, *Eco-friendly decolorization and degradation of reactive yellow 145 textile dye by Pseudomonas aeruginosa and Thiosphaera pantotropha*. Journal of environmental management, 2020. 263: p. 110383.
29. Huang, Y., C. Qiu, Y. Wang, et al., *Effect of tea polyphenols on the fermentation quality, protein preservation, antioxidant capacity and bacterial community of stylo silage*. Frontiers in Microbiology, 2022. 13: p. 993750.
30. Zeng, Q., S. Lu, X. Li, et al., *Bioactive Ingredients and Microbial Diversity of Fuzhuan Tea Produced from Different Raw Materials*. Food Science, 2020. 41(24): p. 69–77.
31. Chen, G., Z. Zeng, M. Xie, et al., *Fermentation characteristics and probiotic activity of a purified fraction of polysaccharides from Fuzhuan brick tea*. Food Science and Human Wellness, 2022. 11(3): p. 727–737.
32. Wang, Y., X. Qiu, and W. Xu, *Response Surface Optimization of Vat Blue 4 Degradation Process Using Pseudomonas aeruginosa WYT*. Polish Journal of Environmental Studies, 2023. 32(1).
33. Tacas, A.C.J., P.-W. Tsai, L.L. Tayo, et al., *Degradation and biotoxicity of azo dyes using indigenous bacteria-acclimated microbial fuel cells (MFCs)*. Process Biochemistry, 2021. 102: p. 59–71.
34. Chantarasiri, A., *Klebsiella and Enterobacter isolated from mangrove wetland soils in Thailand and their application in biological decolorization of textile reactive dyes*. International Journal of Environmental Research and Public Health, 2020. 17(20): p. 7531.
35. Galai, S., A. Perez de los Rios, F.J. Hernández-Fernández, et al., *Microbial fuel cell application for azoic dye decolorization with simultaneous bioenergy production using Stenotrophomonas sp*. Chemical Engineering & Technology, 2015. 38(9): p. 1511–1518.
36. Wang, J., J. Shen, Y. Wu, et al., *Phylogenetic beta diversity in bacterial assemblages across ecosystems: deterministic versus stochastic processes*. The ISME journal, 2013. 7(7): p. 1310–1321.

37. Akita, H., S. Fujimoto, K. Wada, et al., *Performance of Burkholderia multivorans CCA53 for ethyl red degradation*. The Journal of General and Applied Microbiology, 2020. 66(4): p. 220–227.

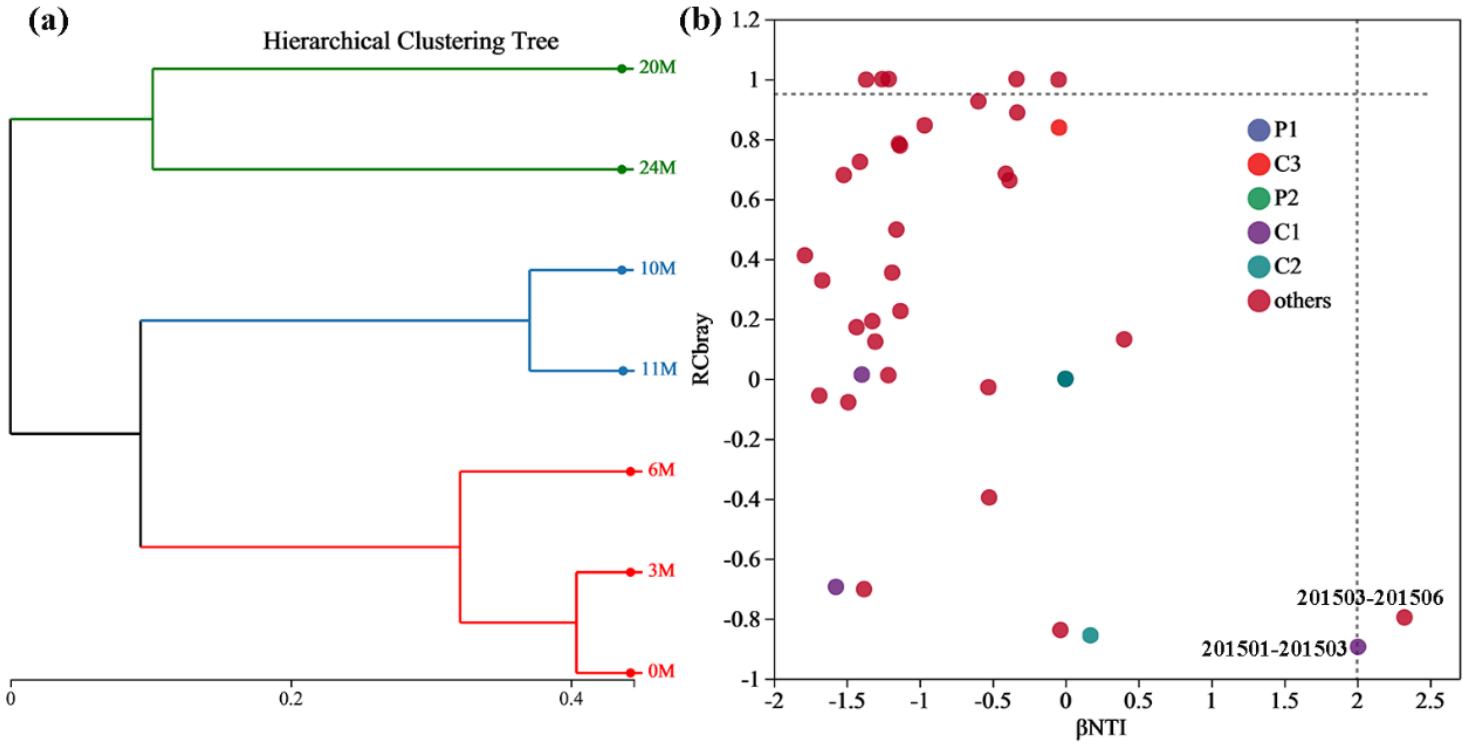
38. Gan, L., F. Zhou, G. Owens, et al., *Burkholderia cepacia immobilized on eucalyptus leaves used to simultaneously remove malachite green (MG) and Cr (VI)*. Colloids and Surfaces B: Biointerfaces, 2018. 172: p. 526–531.

## Figures



## Figure 1

Changes in decolorization ratio of functional microbiome during prolonged incubation. (a) Decolorization ratio change during DDMY1 domestication and application period, (b) Decolorization ratio change during DDMZ1 domestication and application period, (c) Activator addition to DDMY1 and DDMY2 decolorization ratio change over time, (d) Decolorization ratio time change of functional microbiome DDMZ1 under different types of dye conditions, (e) Decolorization ratio time change of functional microbiome DDMZ1 under different concentrations of dye conditions, (f) Decolorization ratio time change of functional microbiome DDMZ1 under different electron donor conditions.




## Figure 2

Evolutionary map of the microbiome during DDMY1 domestication. (a) Hierarchical clustering tree diagram of the microbiome, (b) βNTI/RCbray community structure analysis. (Different subgroups in the legend represent two-by-two comparisons between samples within different groups, others represent comparisons between samples within different subgroups. c1: initial microbiome vs. 3 months, c2: 3 months vs. 6 months, c3: 6 months vs. 10 months, p1: 11 months vs. 20 months, and P2: 20 months vs. 24 months).

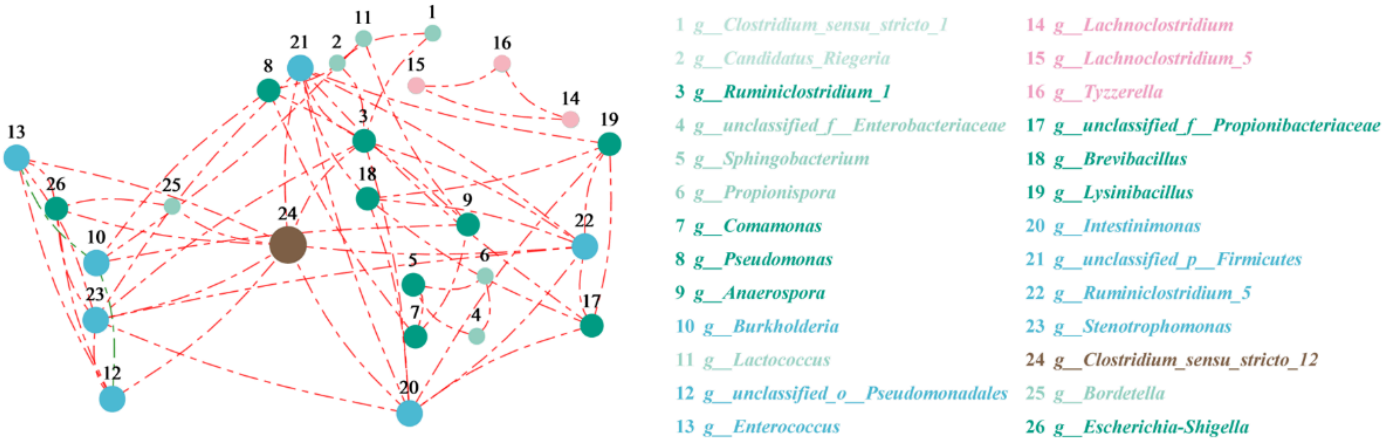
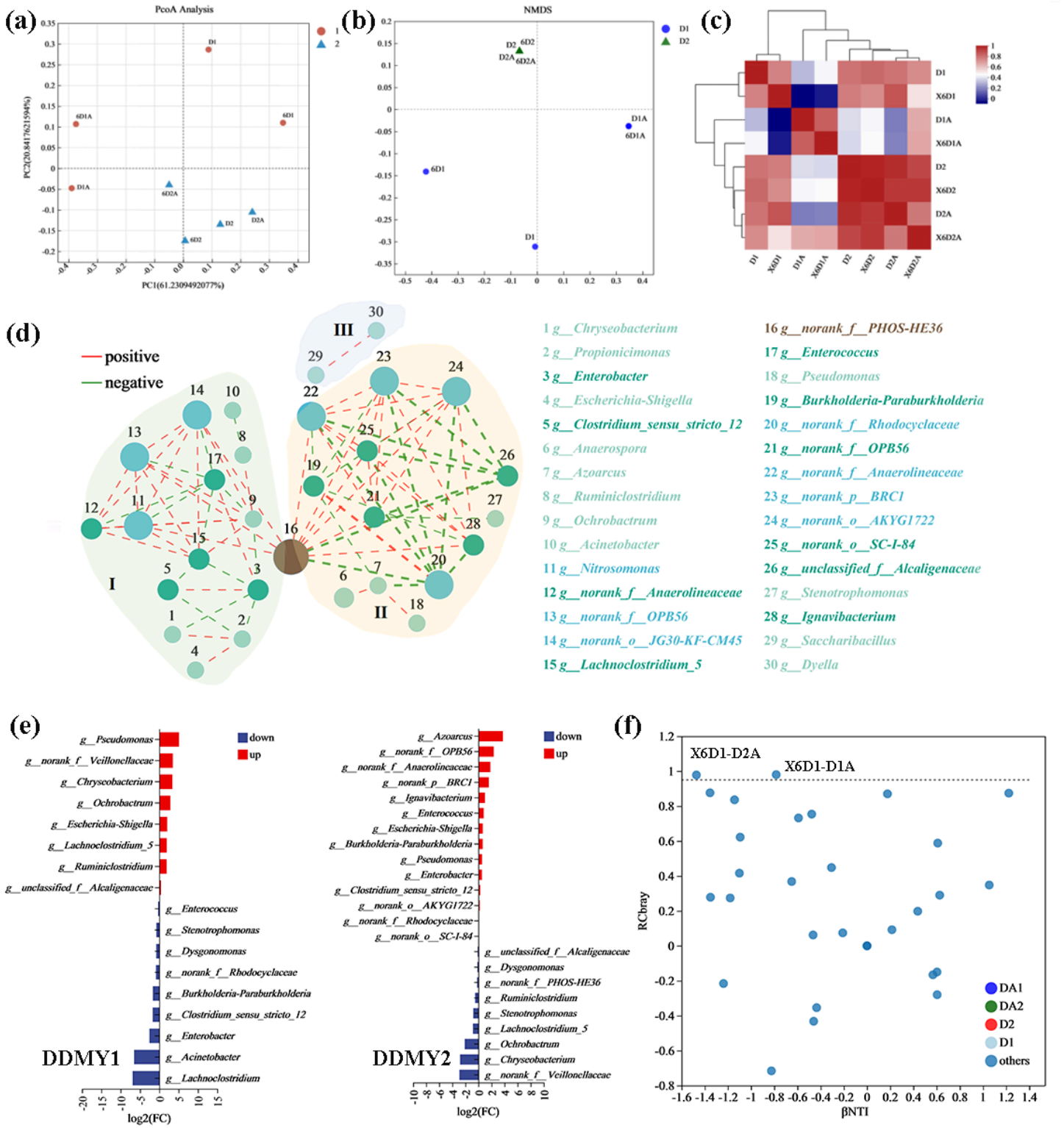



**Figure 3**

Network analysis of functional microbiome DDMY1 network associations during domestication and application.




## Figure 4

Effect of activators on the community structure of functional microbiome. (a) PcoA analysis, (b) NMDS, (c) correlation analysis, (d) Network correlation network analysis, (e) Fold change analysis, (f) βNTI/RCbray community structure analysis. (In (a)(b)(c): D1: DDMY1, 6D1(X6D1): DDMY1 after 6 months of RBBR domestication, D1A:DDMY1+ activator, 6D1A(X6D1A): DDMY1+ activator for 6 months of domestication, D2: DDMY2, 6D2(X6D2): DDMY2 after 6 months of co-domestication of RBBR and tea

residues, D2A: DDMY2+ activator, 6D2A(X6D2A): DDMY2+ activator for 6 months of domestication.) (In (f): D1: DDMY1 after 6 months of RBBR, DA1: DDMY1+ activator and DDMY1+ activator for 6 months of domestication, D2: DDMY2 after 6 months of co-domestication of RBBR and tea residues, DA2: DDMY2+ activator and DDMY2+ activator for 6 months of domestication).

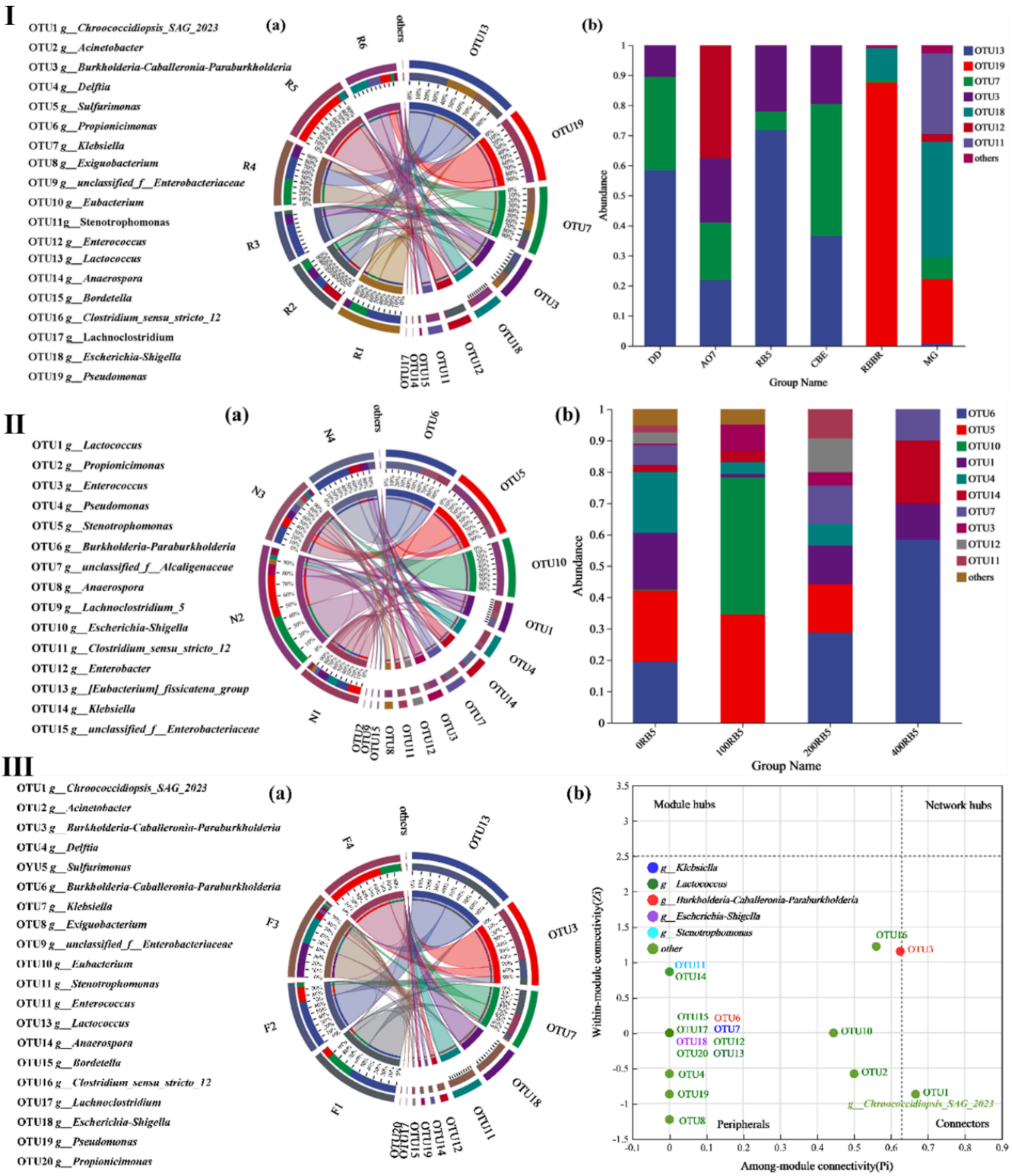



**Figure 5**

Influence of environmental factors on the community structure of functional microbiome. (I. Effects of different structural types of dye electron acceptors on the community structure of functional microbiome. (a) Circos plot, (b) stacked bar graph. (R1: DDMZ1, R2:DDMZ1+AO7, R3:DDMZ1+RB5, R4:DDMZ1+CBE, R5:DDMZ1+RBBR, R6:DDMZ1+MG)), (II. Effect of different concentrations of dyes on the community structure of functional microbiome. (a) Circos plot, (b) Stacked bar graph. (N1: DDMZ1, N2: DDMZ1+100 mg/L RB5, N3:DDMZ1+200 mg/L RB5, N4:DDMZ1+400 mg/L RB5)), (III. Effects of different electron donors on the community structure of functional microbiome. (a) Circos plot, (b) ZIPI analysis. (F1：YE, F2：MN, F3:FRU, F4: YE+FRU)).

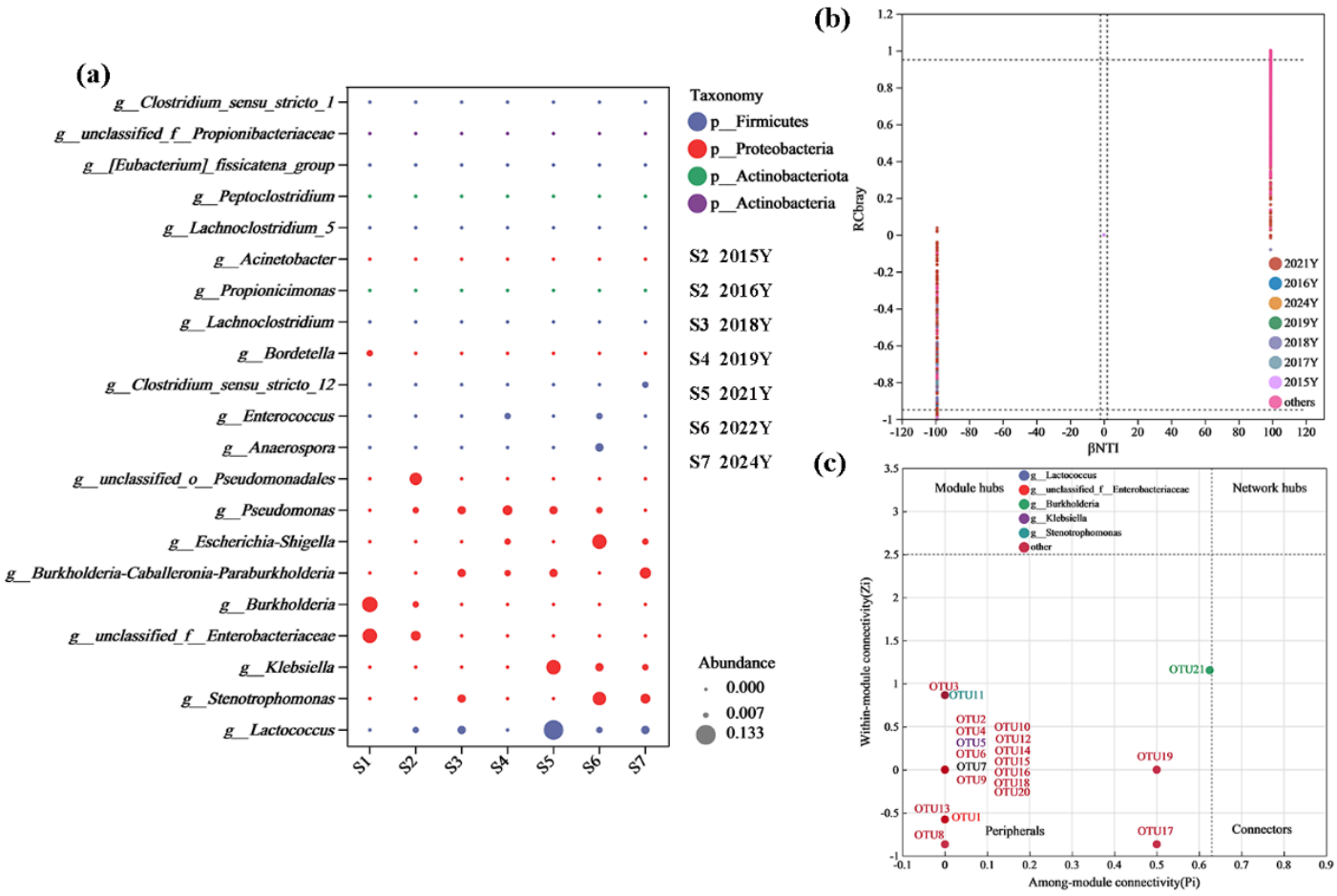



**Figure 6**

Evolutionary studies of functional microbiome over a decade. (a) Bubble plot of community abundance, (b) βNTI/RCbray community structure analysis. (Different groupings in the legend represent two-by-two comparisons between samples within different groups, and others represent comparisons between samples within different groupings), (c) ZIPI analysis.

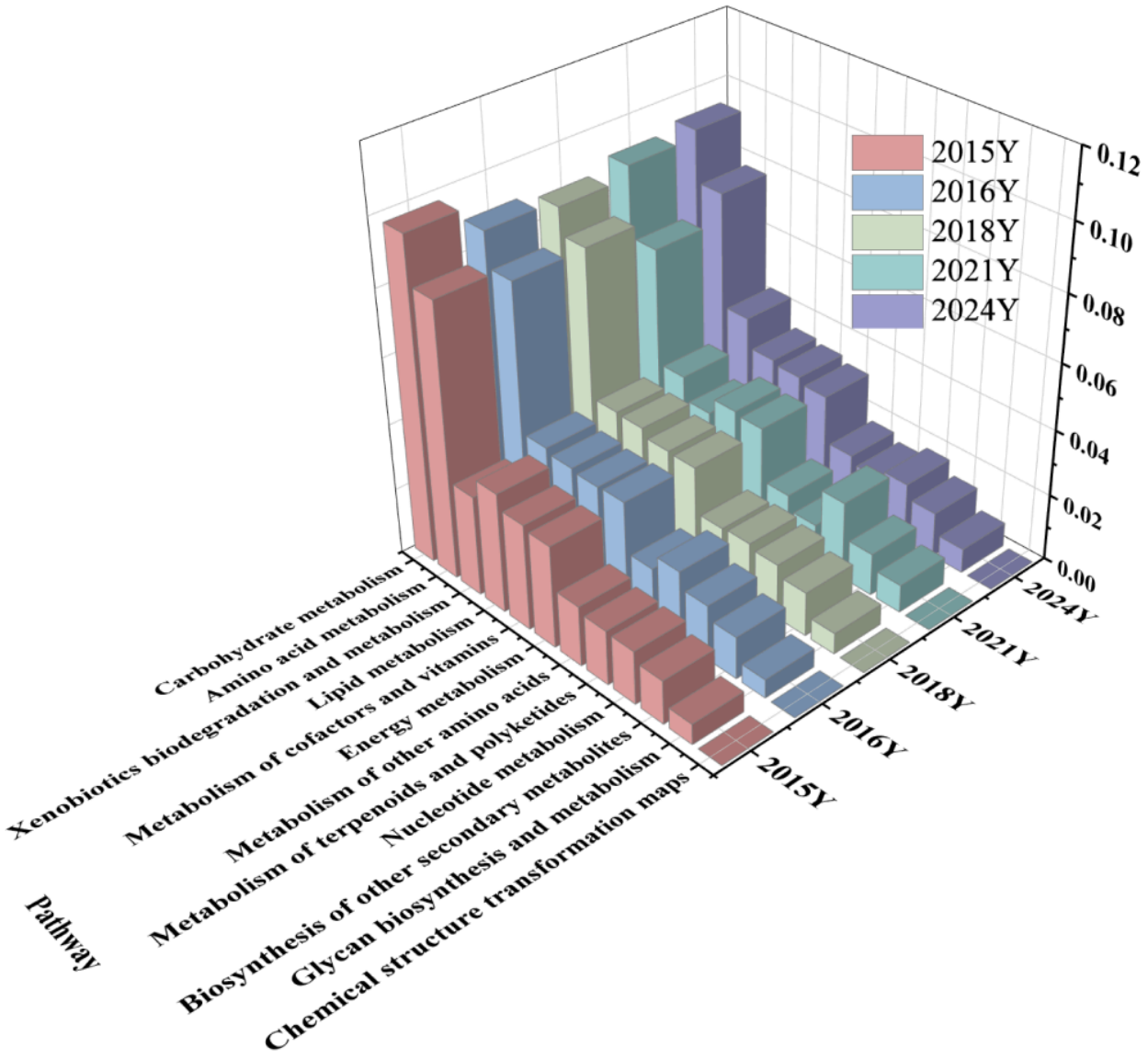



**Figure 7**

Graph of decadal variation study of predictive function of microbial community (Metabolism level).